

Sustainable Metallographic Preparation: Specific Case of Nickel Aluminium Bronze (NAB), Manganese Aluminium Bronze (MAB) and a Duplex Brass

María Victoria Biezma Moraleda^{a, *}, Lourdes Merino Galván^a,
José Fernández Palacio^b, Carlos Berlanga Labari^c

^aUniversidad de Cantabria, Dpt. de Ciencia e Ingeniería del Terreno y de los Materiales. España

^bAsociación de la Industria Navarra (AIN), Spain and Public University of Navarre (UPNA),
Dpt. Materials Science and Metallurgical Engineering, Spain

^cPublic University of Navarre (UPNA), Dpt. Materials Science and Metallurgical Engineering, Spain

(*Corresponding author: biezmav@unican.es)

Submitted: 13 November 2024; Accepted: 23 September 2025; Available On-line: 19 November 2025

ABSTRACT: Nickel Aluminium Bronze (NAB) and Manganese Aluminium Bronze (MAB) are highly alloyed metallic systems that are widely used in naval applications due to their excellent corrosion resistance and mechanical and tribological properties, such as cavitation and erosion resistance. Duplex brass is also an excellent option due to its ability to increase mechanical properties and corrosion resistance by selected thermal treatments. Chemical reagents currently used for metallography in research laboratories and in industry, are based mainly upon acidic iron chloride solutions. This work shows the results of microstructural features of these alloys after grinding and polishing of selected specimens in as cast state, with alumina or diamond paste of different sizes, using tap water and distilled water. The main conclusion is that the microstructure of these materials is perfectly revealed without the usual etching step involving a chemical reagent, thus reducing both the environmental and the economic impact.

KEYWORDS: Brass; Bronze; Etching; Metallography; Microstructure; Polishing

Citation/Citar como: Biezma Moraleda, M.V.; Merino Galván, L.; Fernandez Palacio, J.; Berlanga Labari, C. (2025). "Sustainable Metallographic Preparation: Specific Case of Nickel Aluminium Bronze (NAB), Manganese Aluminium Bronze (MAB) and a Duplex Brass". *Rev. Metal.* 60(4): e271. <https://doi.org/10.3989/revmetalm.e271.1651>

RESUMEN: *Preparación metalográfica sostenible: Casos particulares en un bronce al níquel y aluminio (NAB), un bronce al manganeso y aluminio, (MAB) y un latón duplex.* El bronce al níquel y aluminio (NAB) y el bronce al manganeso y aluminio (MAB) son sistemas metálicos altamente aleados, y ampliamente utilizados en aplicaciones navales, debido a su excelente resistencia a la corrosión, así como excelentes propiedades mecánicas y tribológicas (resistencia a la cavitación y la erosión). El latón dúplex también es una excelente opción, debido a su capacidad para mejorar las propiedades mecánicas y la resistencia a la corrosión mediante tratamientos térmicos específicos. Los reactivos químicos utilizados actualmente en metalografía, tanto en laboratorios de investigación como en la industria, se basan principalmente en soluciones ácidas de cloruro de hierro. Este trabajo muestra los resultados de la caracterización microestructural de estas aleaciones, en estado de colada, tras el desbaste y pulido, con pasta de alúmina o diamante de diferentes tamaños, utilizando agua corriente y agua destilada. La principal conclusión es que la microestructura de estos materiales se revela perfectamente sin la etapa habitual de ataque con reactivo químico, lo que reduce, tanto el impacto ambiental como el económico.

PALABRAS CLAVE: Ataque Químico; Bronce; Latón; Metalografía; Microestructura; Pulido

ORCID ID: María Victoria Biezma Moraleda (<https://orcid.org/0000-0002-0709-7656>); Lourdes Merino Galván (<https://orcid.org/0009-0003-3630-847X>); José Fernández Palacio (<https://orcid.org/0000-0002-7479-8655>); Carlos Berlanga Labari (<https://orcid.org/0000-0002-7069-3768>)

1. INTRODUCTION

Copper-based alloys are widely used in different sectors of the industry for the manufacturing of different components such as valves, propellers, impellers, tubes or bearings due to the elevated physical-chemical properties of bronzes with a high resistance to cavitation or erosion, as well as a high corrosion resistance. Brass also excels in the easiness for machining, showing both high thermal and electrical conductivity together with high wear and corrosion resistance (Song *et al.*, 2017; Al-Hashem and Riad, 2002).

Highly alloyed bronzes such as Nickel-Aluminium Bronze (NAB) or Manganese-Aluminium Bronze (MAB) happen to be the main alloys for the manufacturing of rotating elements such as pump impellers or propellers for the naval industry or for many components in the aerospace industry (Richardson, 2016). These two alloys are characterized by a complex multi-phased microstructure where α (α), β (β) and κ (κ) are well differentiated, although the chemical composition, geometry, size, distribution and the number of phases is different for each of the systems (Linhardt *et al.*, 2021; Cobo *et al.*, 2022).

NAB is composed of mainly copper, with high amounts of nickel, aluminium and iron, where the two first elements increase the mechanical properties while the iron reduces the grain size and therefore, the ultimate tensile strength gets enhanced. At high temperatures, the β -phase with bcc structure is formed, which is then transformed into α -phase (fcc) intercalated with four κ precipitates showing bcc structure. The microstructure is sensitive to compositional changes and to heat treatments (Tian *et al.*, 2022; Berlanga Labari *et al.*, 2023; Cobo *et al.*, 2022).

The intermetallic compounds are κ_I and κ_{II} and they can be mistaken. They are either in the α phase or within the interface α/β . κ_I -phase (Fe_3Al) normally is appreciated as a rosette or clover shaped precipitate averaging 7.5 μm in diameter. κ_{II} -phase, on its side, corresponds to the precipitates where κ_I -phase nucleates and is smaller, averaging 1.5 μm in diameter, with a dendritic rosette shape that can develop from the grain boundaries of α/β phases. κ_{IV} -phase contains the highest amount of iron (62% approx.), small but with variable sizes, it is distributed in the α phase matrix. Finally, within the β phase matrix, the κ_{III} -phase ($NiAl$) can be seen, showing a eutectoid structure with the typical long and thin lamellae (Orzolek *et al.*, 2022; Basumatary and Wood, 2017; Cobo Ocejó *et al.*, 2022; Qin *et al.*, 2022; Ni *et al.*, 2010). This high microstructural heterogeneity could induce different corrosion problems (Zhang *et al.*, 2018; Zhao *et al.*, 2020).

In the as cast state, MAB, like NAB, contains a main fcc α -phase with high Cu content, a bcc β -phase and all the κ -phases described above but much bigger. In this case, they are intermetallic compounds rich in Fe and Mn, with either fcc or bcc structures (Cobo Ocejó *et al.*, 2022). The main difference between both alloys is the higher content in Mn of this one and to a lesser extent, the differences in Ni and Fe percentages. For this system, as in the previous case, the complex microstructure is a handicap in the performance against corrosion, aggravated in this material by the size of the κ -phases, which act as big cathodes in front of α and β phases when any electrolyte is present. In that scenario, β -phase is prone to corrode by desaluminization as the Al and Mn contents are higher compared to those of the α -phase, while the latter is preferentially corroded compared to κ -phases due to its higher amount of Fe, Al, Ni and Mn (Linhardt *et al.*, 2021; Roy *et al.*, 2018; Mota *et al.*, 2021).

Commercial bronzes are divided into two broad groups, bronzes α , and duplex bronzes α and β . A widely used type of brass, cheaper and with a higher mechanical resistance and higher ductility compared to monophasic brass, is the biphasic or duplex brass which is composed of α and β phases as the one in this study. Both types of bronzes are extensively used in industry, but duplex brass does contain more Zn than the monophasic one, which may induce selective corrosion due to the different galvanic potential between the phases, thus developing what is known as dezincification of brass, affecting more to the β -phase (Lazar *et al.*, 2019; Mora Pozo and Venegas Ledo, 2011).

Brass also shows both a high thermal and electrical conductivity together with high wear and corrosion resistance excels in the easiness for machining. Moreover, they show an ability to increase mechanical properties and the resistance to corrosion as well cavitation erosion by selected thermal treatment and/or alloy (Lazar *et al.*, 2021).

Regarding the etching of these materials, Biezma (2022) compiled the most used chemical etchants for NAB and MAB alloys, highlighting that the majority are based on ferric chloride (FeCl_3), applied in either water- or alcohol-based solutions. Other frequently used reagents include nitric acid (HNO_3), ammonium chloride (NH_4Cl), ammonium persulphate ($(\text{NH}_4)_2\text{S}_2\text{O}_8$), and ammonium hydroxide (NH_4OH), in various compound formulations. These options are discussed throughout the manuscript in connection with their effectiveness in revealing specific microstructural features. Classical metallography references, such as Voort (2004), also recommend these etchants for copper-based alloys. Among them, ferric chloride and cupric ammonium chloride ($(\text{NH}_4)_2\text{CuCl}_4$) remain the most widely applied for general microstructural contrast.

In the case of brass alloys, the most commonly used reagents include cupric ammonium chloride ($(\text{NH}_4)_2\text{CuCl}_4$) and Klemm's Reagent II, as noted in Biezma *et al.* (2023). Additionally, recent studies have demonstrated the use of acidic ferric chloride to distinguish α and β' phases in duplex brasses (Moriarty *et al.*, 2021), or saturated sodium thiosulphate solutions (Farabi *et al.*, 2015). Another study by Gregg (1990) employed a solution of nitric acid and distilled water in a 1:1 volumetric ratio for approximately 3 seconds to reveal α -Widmanstätten structures and β phases. Similarly, Khalili *et al.* (2022) reported the successful use of a solution composed of 2 g FeCl_3 , 10 mL distilled water, and 10 mL HCl applied for 6 seconds, enabling distinction between α grains and β -phase particles, which appeared white and brown, respectively.

The primary difference between the etchants used in the present work (FeCl_3 -based, in both water and alcohol media) and those reported in the literature lies in the resulting coloration of the microstructure, rather than in etching effectiveness. In both cases, high-quality microstructural resolution can be achieved, as demonstrated in the current study.

The main aim of the present work is to show how the metallographic preparation, after grinding and polishing using different abrasives, alumina and/or diamond paste of different grain sizes in a manual polishing machine, and using tap water as cooling media, can clearly reveal the microstructure of the selected copper bases alloys without using any chemical reagent. For comparison purposes, and with the aim of determining the influence of the electrolyte itself together with the abrasive material, also distilled water was used. These facts have a clear environmental and economic impact in laboratories, due to the non-use of chemicals and the reduction in time for specimen's preparation.

2. MATERIALS AND METHODS

Two highly bronzed in as cast condition, NAB (C96500) and MAB (C95400), and a brass, CB771S, were used in this study. Their chemical compositions are shown in Table 1.

Specimens of ca. 20x20x3 mm³ were cut from ingots and the surface preparation of the samples was assessed by grinding with silicon carbide papers from grit 80 to 1000, followed by a comparative study of four different polishing procedures, all carried out in a manual polishing machine.

- Procedure 1: Alumina paste from 1 to 0.5 μm , using tap water as cooling media.
- Procedure 2: Diamond paste from 6 to 1 μm as abrasive, using tap water as cooling media.
- Procedure 3: Hybrid way with two steps: first alumina paste and then diamond paste, both of 1 μm , using tap water as cooling media.
- Procedure 4: Similar to 3 but using distilled water instead of tap water.

The alumina paste employed in procedures 1, 3 and 4 was a 99% pure agglomerated alpha-alumina suspension (Alumina AP-D), supplied by Struers. It was prepared using distilled water.

No information was provided regarding the presence of additives commonly used to enhance the wettability or erosive properties of polishing pastes—such as stearic acid, paraffin, lime, ethyl alcohol, oleic acid, chromic oxide, aluminium oxide, white mud, feldspar powder, oils, hardened oils, or polyethylene glycol.

It is important to note that stearic acid and other compounds with long polymer chains, such as oleic acid, are recognized corrosion inhibitors. These substances are often employed—either alone or in combination with other acids and/or oils—to promote the formation of protective layers on bronzes and other copper-based alloys, as reported in the literature (Han *et al.*, 2024; Markusi *et al.*, 2015; Abdel-Karim and El-Shamy, 2022).

TABLE 1. Chemical composition of the different alloys (bulk) and the phases within them (%wt.)

	Phase	Cu	Fe	Al	Ni	Mn	Zn	Pb	Sn	Si
NAB - C96500	Bulk	79.8	4.9	9.3	4.6	1.2	0.05	0.006	0.006	0.04
	α	79.1	2.9	9.3	5.6	1.1	N.A.	N.A.	N.A.	N.A.
	β	70.5	15.5	6.4	3.3	1.2	N.A.	N.A.	N.A.	N.A.
	κ _I (Fe ₃ Al)	7.1	64.6	13.3	16.8	2.7	N.A.	N.A.	N.A.	N.A.
	κ _{II}	12.9	63.9	11.6	12.6	1.6	N.A.	N.A.	N.A.	N.A.
	κ _{III} (NiAl)	58.5	3.9	13.1	13.8	1.4	N.A.	N.A.	N.A.	N.A.
	κ _{IV} [2]	13 ± 1	4 ± 1	20 ± 3	62 ± 4	1.5 ± 0.3	N.A.	N.A.	N.A.	N.A.
MAB - C95400	Bulk	70.9	4.6	7.1	2.0	12.6	2.3	0.013	0.006	0.03
	α	74.9	1.9	7.7	1.4	11.4	N.A.	N.A.	N.A.	N.A.
	β	59.5	2.6	12.6	6.4	17.0	N.A.	N.A.	N.A.	N.A.
	κ	9.8	57.7	7.5	1.7	21.9	N.A.	N.A.	N.A.	N.A.
BRASS CB771S	Bulk	62.3	0.1	0.6	0.1	-	≈ 37	0.19	0.04	0.004
	α (dark)	64.3	-	-	-	-	35.7	N.A.	N.A.	N.A.
	β	58.4	-	1.1	-	-	40.5	N.A.	N.A.	N.A.

For the final polishing stages of procedure 2, both polycrystalline and monocrystalline (also in procedures 3 and 4) diamond abrasives were employed. Specifically, diamond sprays M (1 μm, monocrystalline), P (3 μm), and X (6 μm, polycrystalline) were used (Struers M, P, and X series, respectively).

In addition, a diamond suspension DP-P, 3 μm (polycrystalline), was applied. This suspension consists of diamond particles dispersed in an alcohol-based medium that includes 5-chloro-2-methyl-4-isothiazolin-3-one (EC No. 247-500-7) and 2-methyl-2H-isothiazol-3-one (EC No. 220-239-6) in a 3:1 ratio, as specified by the product manufacturer.

In all final polishing stages of the studied alloys (NAB, MAB, and brass), a 3 μm polycrystalline diamond suspension was consistently employed prior to the final polishing steps with finer abrasives.

The chemical composition of the tap water in the city of Santander, Spain (www.aqualia.com), where the study was carried out, and used for procedures 1 to 3, is presented in Table 2.

TABLE 2. Chemical composition of the tap water in Santander

Element	Measure
pH	7.58
Calcium + Magnesium	<300 mg·L ⁻¹
Bicarbonate	Aprox. 300 mg·L ⁻¹
Chlorides	62.7 mg·L ⁻¹
Sulphates	124 mg·L ⁻¹
Manganese	< 2.5 μg·L ⁻¹
Free residual chlorine	0.88 mg·L ⁻¹
Sodium	35.8 mg·L ⁻¹
Aluminium	54.2 μg·L ⁻¹

As for distilled water, conductivity is the most relevant parameter. The pH is primarily determined by the amount of dissolved CO₂ from the ambient air. Given the high purity of distilled water, ionic concentrations are extremely low—below the detection limits of standard analytical methods. Therefore, conductivity is typically used as an integral indicator of purity. According to the supplier's specification at the time of storage, the conductivity was reported as < 1 µS/cm at 20 °C, with a pH ranging from 4.5 to 8.

Finally, to enable comparison between the different polishing procedures and the effects of etching, two ferric chloride solutions (reagents 1 and 2) were applied for 10 seconds—an etching time commonly reported in the literature (Voort, 2004; Böhm *et al.*, 2019) and consistent with the typical 5–15 second range for copper-based alloys (Cobo *et al.*, 2022)—as an average value selected to prevent overetching, particularly given the high surface reactivity of these materials immediately after polishing, as observed throughout our experimental work.

- Reagent 1 (R1): 5 g of iron chloride, FeCl₃, 20 ml HCl and 80 ml of distilled water (Linhardt *et al.*, 2021; Cobo Ocejo *et al.*, 2022)
- Reagent 2 (R2): 5 g of iron chloride FeCl₃, 2 ml of HCl, 95 ml of ethanol C₂H₆O (Wu *et al.*, 2015; Yao and Shim, 2022).

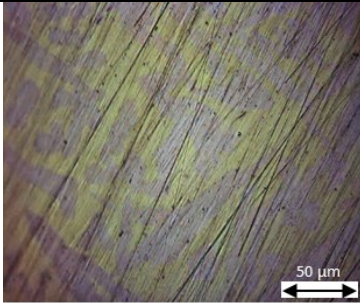
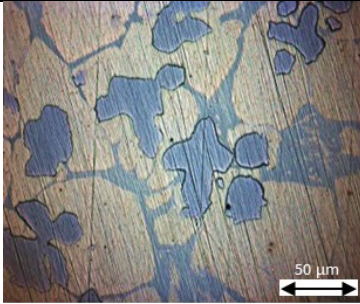
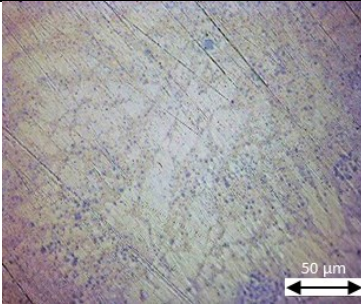
A Leica DM4000 M optical microscope in bright field mode was used for assessing the metallographic study. Samples of each of the alloys have been analysed in a Zeiss Evo MA15 Scanning Electron Microscope (SEM), and the chemical composition of the different phases have been evaluated by means of an energy dispersive X-rays analyser (EDX).

3. RESULTS

Table 1 summarizes the chemical composition (%wt.) for the bulk of NAB, MAB and brass, respectively, together with the composition (%wt) of the phases separately by means of the EDX.

Table 3 shows the evolution of the different microstructures after polishing during 10 minutes with alumina paste of different sizes, from 1 µm to 0.05 µm, for the selected materials.

TABLE 3. Microstructure characterization of brass, MAB and NAB using alumina paste of 1 µm, 0.25 µm and 0.05 µm as a final polishing step and tap water as a cooling media

Alumina paste			
Polishing	BRASS	MAB	NAB
1 µm			

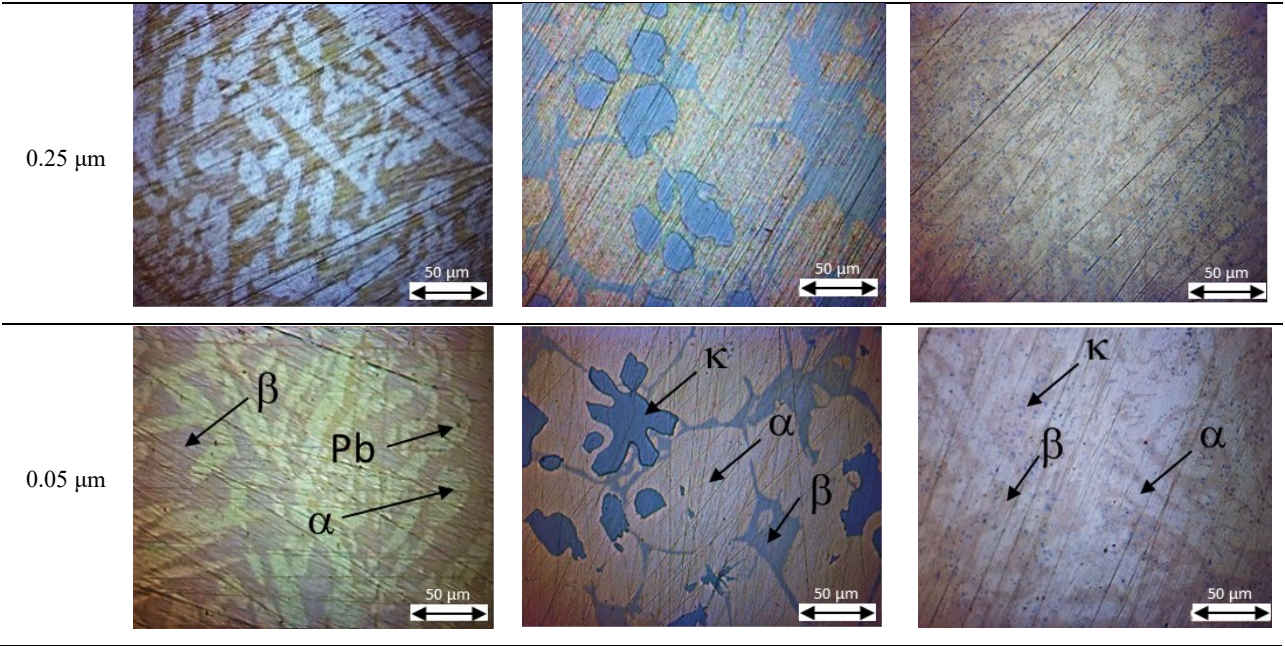
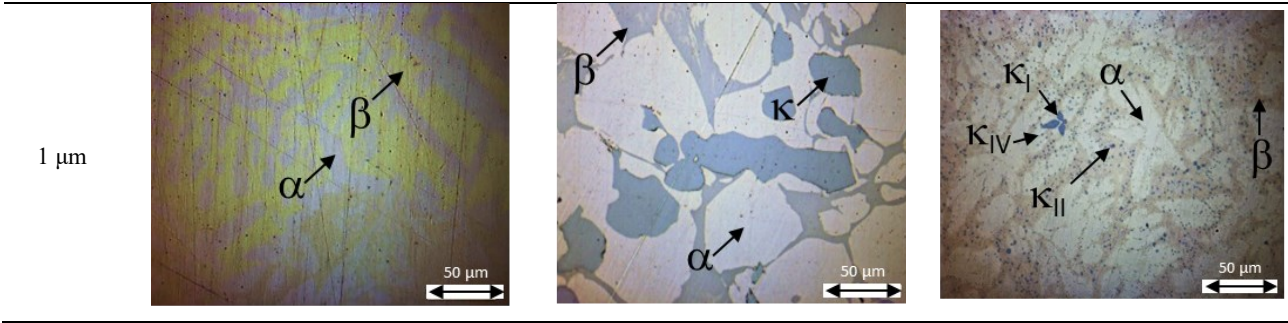


Table 4 shows the evolution of the different microstructures after being polished for 10 minutes with diamond paste of different granulometries, from 6 μm to 1 μm, for the selected materials. In particular, the last row has been used to identify the main phases of the three studied materials.

TABLE 4. Microstructure characterization of brass, MAB and NAB using diamond paste of 6 μm, 3 μm and 1 μm as a final polishing step and tap water as a cooling media

Diamond paste			
Polishing	BRASS	MAB	NAB
6 μm			
3 μm			



In Tables 5 and 6, shows the evolution of the different microstructures after being polished, firstly using alumina paste of 1 µm for 10 minutes, and final polishing using diamond paste of different sizes, from 6 µm to 1 µm, using tap water and distilled water respectively.

TABLE 5. Microstructure characterization of brass, MAB and NAB magnification using firstly alumina paste of 1 µm (x200), and then diamond paste of 6 µm, 3 µm and 1 µm with tap water as a cooling media

Alumina paste			
Polishing	BRASS	MAB	NAB
1 µm			
Diamond paste			
6 µm			
3 µm			

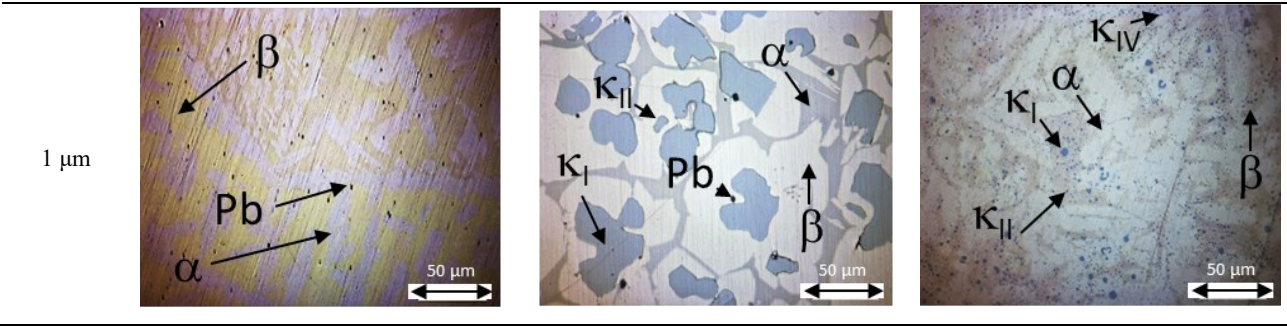
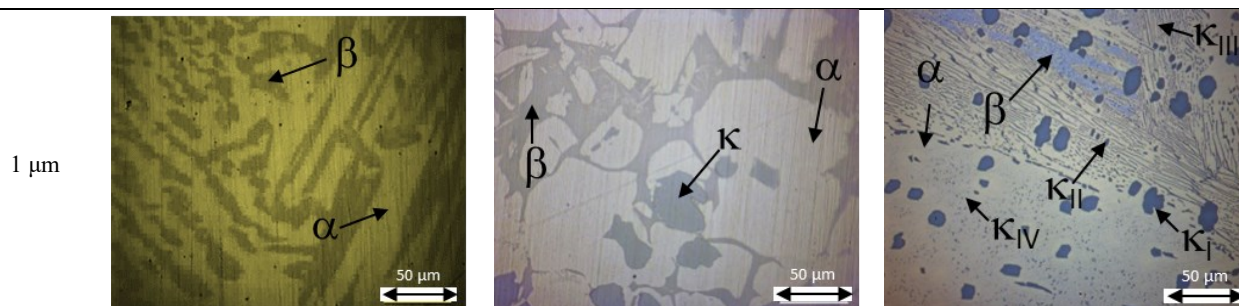


TABLE 6. Microstructure characterization of brass, MAB and NAB using firstly alumina paste of 1 μm , and then diamond paste of 6 μm , 3 μm and 1 μm , using distilled water

Alumina paste			
Polishing	BRASS	MAB	NAB
1 μm			
Diamond paste			
6 μm			
3 μm			



A careful observation of the results allows to confirm that the use of the different polishing procedures carried out during this study is suitable to reveal microstructure of the selected materials. Some important observations to point out: alumina is a very good polishing abrasive for these materials; it needs shorter times to remove the material but smaller polishing size, 0.25 and 0.05 μm , is required to leave a uniform surface to remove scratches. This fact is especially relevant on brasses where the abrasive is too hard and does not leave a surface finish as good as that of the diamond paste. Diamond paste therefore leaves a low level of scratches, is less abrasive to the κ -phases but it needs longer times, around 30 minutes, to reach a similar surface state as alumina, especially for duplex brass. Finally, it turns out that the hybrid procedure, alumina pastes and diamond, optimises the results. The hybrid procedure offers high performance considering that the specimen surface has no scratches permitting resolving the microstructure with less abrasive compounds.

MAB is the material with the best microstructural definition, including both abrasives with higher grain size, and it clearly permits to identify the three phases, α , β and κ , with a typical rosette and or petal shape, as it was indicated for each procedure. Brasses present the handicap of the mechanical resistance and the difficulty to remove all scratches, but the microstructure, formed by α and β phases since is a duplex brass, can still be identified. Moreover, it has been observed from the first stages of each procedure, and visible at even the lower magnifications. NAB is the most penalized material in comparison to MAB due to the lower size of their phases that avoid an optimum definition, in particular the κ phases.

4. DISCUSSION

Both cooling agents permit to reveal the microstructure with similar definition. The chemical composition of tap water (Table 2) typically includes essential components such as chlorine, chloride, bicarbonate, fluoride, nitrate, sulphate, phosphate, sodium, potassium, magnesium, calcium, iron, and manganese. The ability of the polishing system to reveal the microstructure is therefore presumably related not only to the erosive action of alumina—particularly evident in NAB and MAB bronzes due to the presence of intermetallic phases embedded within the copper-rich α -phase or at α/β interfaces (as in the case of the KIII phase in NAB)—but also to the chemical interactions with certain components of the tap water.


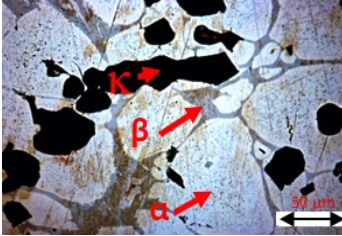
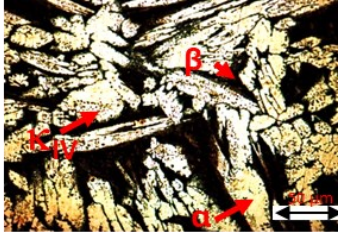
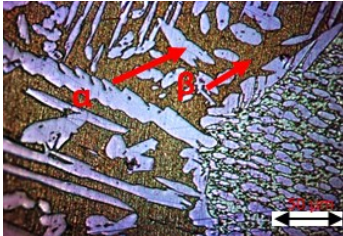
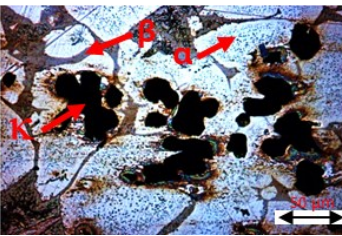
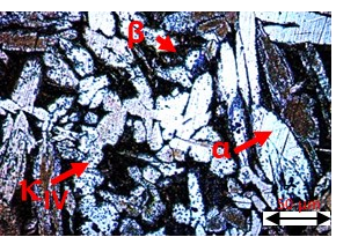
Among the constituents of tap water, chloride, sulphate, and carbonate ions are likely to play a relevant role. Previous studies have shown that in the presence of chloride ions, copper and brass are susceptible to pitting corrosion, although this phenomenon is strongly dependent on chloride concentration (Procaccini *et al.*, 2013). However, tests carried out using tap water confirm that brass alloys can develop a stable and protective surface layer under typical potable water conditions (Gorovei and Benea, 2018). This protective behavior is generally lost in stagnant or highly contaminated waters with elevated chloride content, which is not the case in the present study.

This fact leads to the predominance of the abrasive effect of grinding and polishing steps compared to the effect of the electrolyte as responsible of localized chemical attack to reveal each particular phase (for example, Table 5 and Table 6 for MAB). So, the effect of refrigerant during polishing procedure permits to confirm that the key factor in the revealing of the microstructure is the abrasive effect since procedure 4, that uses distilled water instead of tap water, offers also a good microstructural resolution also for MAB, NAB and brasses. Nevertheless, it is important to point out that κ -phases are less affected by the use of distilled water in MAB meanwhile in NAB the effect is the opposite. NAB and MAB coupons offer the κ -phases with a bluish colour, being brighter after procedure 4. It may be linked with the chemical composition of the protective layer formed on each particular phase (Cobo *et al.*, 2022). Previous studies have shown that cavitation in different electrolytes is able to perfectly reveal the microstructure.

In brass, this procedure allows to clearly observe both phases, α and β with a good definition of grain boundaries. It can be confirmed that colour metallography, used in this research, helps to visualize the different phases on the alloys studied. The use of tap water and distilled water, as coolants during grinding and polishing, helps to sensitize the material to reveal any microstructural feature as segregation, grain orientation and stress state compared to conventional black and white metallography, in agreement with previous works (Dinaharan and Akinlabi, 2017).

Table 7 presents the microstructures of selected materials after chemical etching with the purpose of comparing with non-etched specimens.

TABLE 7. Microstructures of brass, MAB and NAB after chemical etching

	Brass	MAB	NAB
R1 FeCl ₃ + H ₂ O			
R2 FeCl ₃ + Ethanol			

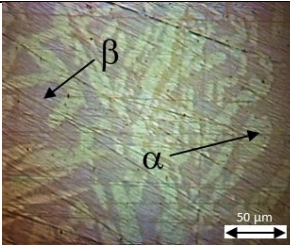
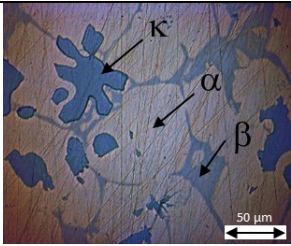
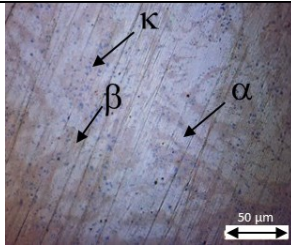
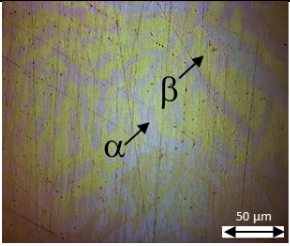
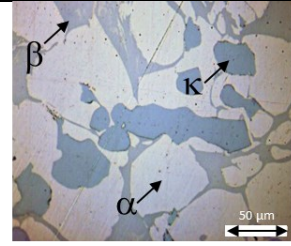
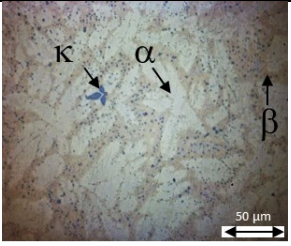
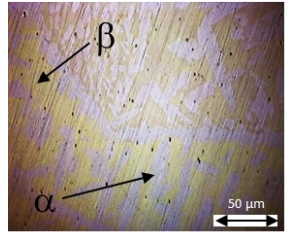
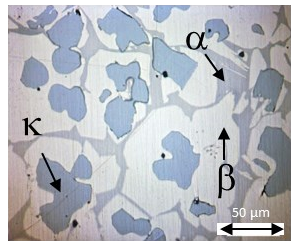
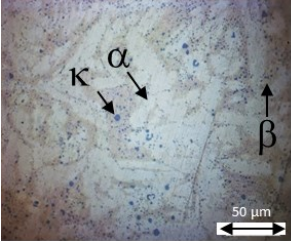
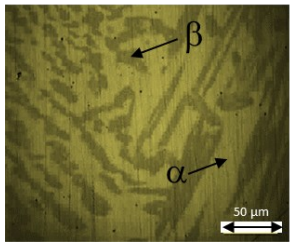
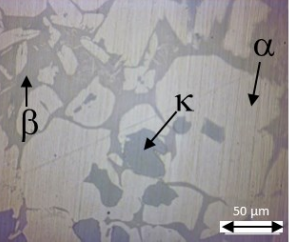
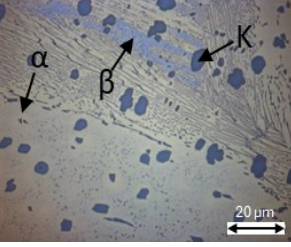
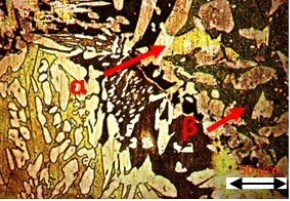
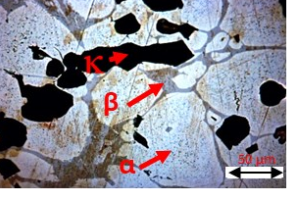
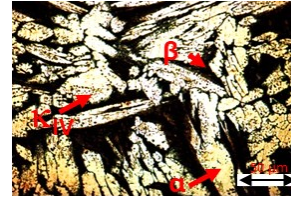
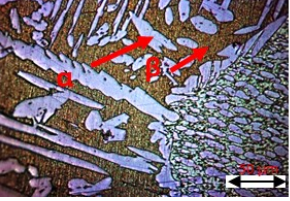
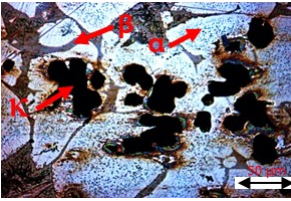
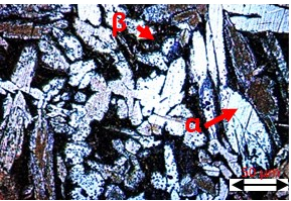
The chemical etching offers a more colourful microstructures of brasses as NAB, and a clear attack due to a strong chemical reaction of κ phases of MAB, in particular with R2, compared to procedures without chemical agents. The appearances of these big κ -phases are dirty, with a halo of corrosion products, and it has been also observed that some κ -phases are removed, with holes left behind appearing as black stains. Based on previous experience, an etching time of 10 seconds seems to be optimal and careful cleaning with alcohol or water before microstructural observation is needed, implying more time in comparison with non-etching procedures. Shorter durations, such as 5 seconds, proved insufficient to achieve adequate contrast between α and β phase grain boundaries in NAB, MAB, and brass, although it tends to prevent the formation of halos around κ (kappa) phases.

MAB alloys contain κ phases enriched in Fe and Mn, which exhibit a pronounced topographical contrast with the surrounding α phase (Rivero *et al.*, 2021). Prolonged etching times can lead to deeper chemical attack at the α/κ interfaces, where the etchant tends to accumulate. This results in localized damage that resembles crevice corrosion and gives the microstructure a corroded or discoloured appearance.

A previous study has shown that a cavitation effect on MAB may perfectly reveal the microstructure, in short time, when exposed to sea water (Biezma *et al.*, 2022; Linhardt *et al.*, 2023).

The use of a chemical reagent in NAB darkens the β phase and does not allow to observe the κ -phases clearly, in opposition to the regular polishing procedure with tap or distilled water. This proves that the possibility of clearly observing the different phases of selected materials depends on the chemistry of each phase and its hardness, related to its resistance to erosion during polishing; it may be worse by the high susceptibility to selective corrosion of these alloys. Table 8 summarizes all the results from the different practical metallographic procedures selected.

TABLE 8. Summary of the microstructures of materials using all defined procedures

Procedure	Brass	MAB	NAB
1 Alumina (A) 0.05 µm			
2 Diamond (D) 1 µm			
3 A+D 1 µm			
4 A+D 1 µm			
R1			
R2			

5. CONCLUSIONS

- Regular polishing using tap water is demonstrated to be very effective for revealing the microstructure of copper alloys. A synergistic combination of the mechanical erosive action of mono- and polycrystalline diamond particles, the chemical contribution of the alcohol-based DP suspension, and the ionic composition of tap water—particularly chloride and sulphate ions—has facilitated the observation of well-defined microstructural features in NAB, MAB, and brass alloys. This has allowed clear phase differentiation even without requiring additional chemical or electrochemical etching steps.
- It has been shown that as the time of exposition to the electrolyte is quite critical if the resolution is to be improved such as the granulometry of the abrasive and its hardness.
- The use of distilled water leads to a more homogeneous surface, with a resolution of the phases like the one obtained using tap water, except for brass.
- The proposed procedures by grinding and polishing without chemical etching, simplify the metallography preparation, take less time, lead to a cleaner laboratory environment; in addition, they allow to save money and result in a more environmentally friendly process.

ACKNOWLEDGMENTS

JCNavalips SL, Latones del Carrión, Spain, for providing specimens, and Gobierno de Cantabria, for financial support of project SUBVTC-2021-0024.

AUTHORSHIP CONTRIBUTION

M^a Victoria Biezma: Conceptualization, Funding acquisition, Investigation, Methodology; Writing – review and editing. **Lourdes Merino:** Formal analysis, investigation, visualization and writing the original draft. **José Fernández:** Investigation, visualization, Writing- review and editing. **Carlos Berlanga:** Investigation, Methodology, Writing- review and editing.

REFERENCES

- Abdel-Karim, A.M., El-Shamy, A.M. (2022). A review on green corrosion inhibitors for protection of archaeological metal artifacts. *J. Bio. Tribo. Corros.* 8, 35. <https://doi.org/10.1007/s40735-022-00636-6>.
- Al-Hashem A., Riad, W. (2002). The role of microstructure of nickel–aluminium–bronze alloy on its cavitation corrosion behavior in natural seawater. *Mater. Charact.* 48 (1), 37–41. [https://doi.org/10.1016/S1044-5803\(02\)00196-1](https://doi.org/10.1016/S1044-5803(02)00196-1).
- Basumatary, J., Wood, R.J.K. (2017). Synergistic effects of cavitation erosion and corrosion for nickel aluminium bronze with oxide film in 3.5% NaCl solution. *Wear* 376-377 (Part B), 1286–1297. <https://doi.org/10.1016/j.wear.2017.01.047>.
- Berlanga-Labari, C., Claver, A., Biezma-Moraleda, M.V., Palacio, J.F. (2023). Study of Effect of Nickel Content on Tribocorrosion Behaviour of Nickel–Aluminium–Bronzes (NABs). *Lubricants* 11 (2), 43. <https://doi.org/10.3390/lubricants11020043>.
- Biezma, M.V., Gómez de la Rasilla, O., Haubner, R., Linhardt, P. (2022). Etching of Manganese Aluminum Bronze by Ultrasound in Seawater. *Prakt. Metallogr.* 59 (5), 236-250. <https://doi.org/10.1515/pm-2022-0027>.
- Biezma, M.V., Strobl, S., Linhardt, P., Ball, G., Haubner, R. (2023). Dezincification in cast and heat-treated alpha-beta brass samples. *Prakt. Metallogr.* 60 (10). <https://doi.org/10.1515/pm-2023-1053>.
- Böhm, J., Haubner, R., Linhardt, P., Biezma Moraleda, M.V. (2019). Corrosion behaviour of a heat treated manganese-nickel-aluminium bronze (MAB) in simulated fresh and sea water. 25 *EUROCORR 2019*, Sevilla, Spain. <http://hdl.handle.net/20.500.12708/101178>.
- Cobo, I., Biezma-Moraleda, M.V., Linhardt, P. (2022). Corrosion evaluation of welded nickel aluminum bronze and manganese aluminum bronze in synthetic sea water. *Mater. Corros.* 73 (11), 1788-1799. <https://doi.org/10.1002/maco.202213328>.
- Cobo Ocejo, I., Biezma Moraleda, M.V., Linhardt, P. (2022). Corrosion Behavior of Heat-Treated Nickel-Aluminum Bronze and Manganese-Aluminum Bronze in Natural Waters. *Metals* 12 (3), 380. <https://doi.org/10.3390/met12030380>.
- Dinakaran, I., Akinlabi, E.T. (2017). Application of Color Metallography to Study the Microstructure of Friction Stir-Welded Dual-Phase Brass Using Various Etchants. *Metallogr. Microstruct. Anal.* 6, 99–105. <https://doi.org/10.1007/s13632-017-0337-x>.
- Farabi, E., Zarei-Hanzaki, A., Pishbin, M.H., Moallemi, M. (2015). Rationalization of duplex brass hot deformation behavior: The role of microstructural components. *Mater. Sci. Eng. A* 641, 360-368. <https://doi.org/10.1016/j.msea.2015.06.042>.
- Gorovei, M.C., Benea, L. (2018). The effect of some key changes in the chemistry of water in relation to copper and brass corrosion control. *IOP Conf. Ser.: Mater. Sci. Eng.* 374 (1), 012057. <https://doi.org/10.1088/1757-899X/374/1/012057>.
- Gregg, N.R. (1990). A Microstructural Investigation of a Duplex Chill Cast Brass Grain Refined with Aluminium and Boron. Doctoral dissertation, University of Surrey, UK.
- Han, Z., Huang, X., Chen, J., Chen, J., Zhou, H. (2024). Study on the compounding of cysteine modified Schiff base and decanoic acid as corrosion inhibitors for bronze with patina. *Surf. Interfaces* 46, 103996. <https://doi.org/10.1016/j.surf.2024.103996>.
- Khalili, M., Eivani, A.R., Seyedein, S.H., Jafarian, H.R. (2022). The effect of multi-pass friction stir processing on microstructure and mechanical properties of dual-phase brass alloy. *J. Mater. Res. Technol.* 21, 1177–1195. <https://doi.org/10.1016/j.jmrt.2022.09.069>.
- Lazar, I., Bordeasu, I., Popoviciu, M.O., Mitelea, I., Craciunescu, C.M., Pirvulescu, L.D., Sava, M., Micu, L.M. (2019). Evaluation of the brass CuZn39Pb3 resistance at vibratory cavitation erosion. *IOP Conf. Ser.: Mater. Sci. Eng.* 477 (1), 012002. <https://doi.org/10.1088/1757-899X/477/1/012002>.

- Lazar, I., Bordeasu, I., Pirvulescu, L.D., Hluscu, M., Mitelea, I., Ghera, C. (2021). The behavior to cavitation erosion-corrosion of the CuZn39Pb3 brass structures, obtained by in-depth heat treatments. *J. Phys.: Conf. Ser.* 1781 (1), 012004. <https://doi.org/10.1088/1742-6596/1781/1/012004>.
- Linhardt, P., Strobl, S., Böhm, J., Biezma, M.V., Haubner, R. (2021). Heat Treatment Effect on the Microstructure and the Corrosion Resistance of Manganese-Aluminum Bronzes. *Prakt. Metall.* 58 (2), 72-82. <https://doi.org/10.1515/pm-2020-0004>.
- Linhardt, P., Biezma, M.V., Strobl, S., Haubner, R. (2023). Influence of Cavitation in Seawater on the Etching Attack of Manganese-Aluminum-Bronzes. *Solid State Phenom.* 341 (8), 25-30. <https://doi.org/10.4028/p-7nbo00>.
- Markusi, M., Otmačić Ćurković, H., Hajdari, Z., Kristan, E. (2015). Patinated bronze protection by long chain organic acids. In *EUROCORR 2015* (European Corrosion Congress). p. 1582
- Mora Pozo, E., Venegas Ledo, E. (2011). *Caracterización del Latón*. *Rev. Met.* UTO 30, 57-64.
- Moriarty, M., Wu, Y., Murray, T., Hutchinson, C. (2021). The effect of phase fraction, size and shape on the dezincification of duplex brasses. *Corros. Sci.* 184, 109366. <https://doi.org/10.1016/j.corsci.2021.109366>.
- Mota, N.M., Tavares, S.S.M., do Nascimento, A.M., Zeeman, G., Biezma Moraleda, M.V. (2021). Failure analysis of a butterfly valve made with nickel aluminum Bronze (NAB) and manganese aluminum Bronze (MAB). *Eng. Fail. Anal.* 129, 105732. <https://doi.org/10.1016/j.engfailanal.2021.105732>.
- Ni, D.R., Xiao, B.L., Ma, Z.Y., Qiao, Y.X., Zheng, Y.G. (2010). Corrosion properties of friction–stir processed cast NiAl bronze. *Corros. Sci.* 52 (5), 1610–1617. <https://doi.org/10.1016/j.corsci.2010.02.026>.
- Orzolek, S.M., Semple, J.K., Fisher, C.R. (2022). Influence of processing on the microstructure of nickel aluminum bronze (NAB). *Addit. Manuf.* 56, 102859. <https://doi.org/10.1016/j.addma.2022.102859>.
- Procaccini, R., Schreiner, W.H., Vázquez, M., Ceré, S. (2013). Surface study of films formed on copper and brass at open circuit potential. *Appl. Surf. Sci.* 268, 171-178. <https://doi.org/10.1016/j.apsusc.2012.12.050>.
- Qin, Z., Li, X., Xia, D., Zhang, Y., Feng, C., Wu, Z., Hu, W. (2022). Effect of compressive stress on cavitation erosion-corrosion behavior of nickel-aluminum bronze alloy. *Ultrason. Sonochem.* 89, 106143. <https://doi.org/10.1016/j.ultsonch.2022.106143>.
- Richardson, I. (2016). *Guide to Nickel Aluminum Bronze for Engineers*. Copper Development Association, Publication N° 222. https://copper.org/applications/marine/nickel_al_bronze. (Accessed Sep. 2025)
- Rivero, P.J.; Berlanga, C.; Palacio, J.F.; Biezma-Moraleda, M.V. (2021). Effect of Ti on microstructure, mechanical properties and corrosion behavior of a nickel-aluminum bronze alloy. *Mater. Res.* 24 (2), e20200335. <https://doi.org/10.1590/1980-5373-MR-2020-0335>.
- Roy, S., Coyne, J.M., Novak, J.A., Edwards, M.A. (2018). Flow-induced failure mechanisms of copper pipe in potable water systems. *Corros. Rev.* 36 (5), 449-481. <https://doi.org/10.1515/corrrev-2017-0120>.
- Song, Q.N., Xu, N., Bao, Y.F., Jian, Y.F., Gu, W., Zheng, Y., Qiao, Y.X. (2017). Corrosion and Cavitation Erosion Behaviors of Two Marine Propeller Materials in Clean and Sulfide-Polluted 3.5% NaCl Solutions. *Acta Metall. Sin.* 30 (8), 712–720. <https://doi.org/10.1007/S40195-017-0602-7>.
- Tian, Y., Zhao, H., Yang, R., Liu, X., Li, H., Chen, X. (2022). Effects of Bacillus sp. adhesion on cavitation erosion behaviour of nickel aluminium bronze in artificial seawater. *Wear* 498-499, 204344. <https://doi.org/10.1016/j.wear.2022.204344>.
- Voort, V. (2004). *ASM Handbook, Metallography and Microstructures*. Volume 9, ASM International, Materials Park, OH, USA, pp. 445-463.
- Yao, C.L., Shim, D.S. (2022). Corrosive properties of CuNi2SiCr fabricated through directed energy deposition on a nickel-aluminum bronze substrate. *J. Alloys Compd.* 918, 165776. <https://doi.org/10.1016/j.jallcom.2022.165776>.
- Zhang, B.B., Wang, J.Z., Yan, F. (2018). Load-dependent tribocorrosion behaviour of nickel-aluminium bronze in artificial seawater. *Corros. Sci.* 131, 252–263. <https://doi.org/10.1016/j.corsci.2017.11.028>.
- Zhao, X., Qi, Y., Wang, J., Peng, T., Zhang, Z., Li, K. (2020). Effect of Weld and Surface Defects on the Corrosion Behavior of Nickel Aluminum Bronze in 3.5% NaCl Solution. *Metals* 10 (9), 1227. <https://doi.org/10.3390/met10091227>.
- Wu, Z., Cheng, Y.F., Liu, L., Weijie, L.V., Hu, W. (2015). Effect of heat treatment on microstructure evolution and erosion–corrosion behavior of a nickel–aluminum bronze alloy in chloride solution. *Corros. Sci.* 98, 260–270. <https://doi.org/10.1016/j.corsci.2015.05.037>.